



HAL
open science

High refractive index IR lenses based on chalcogenide glasses molded by spark plasma sintering

V. Reux, Laurent Calvez, S. Billon, A. Gautier, H.-L. Ma, Patrick Houizot, F. Charpentier, H. Tariel, Z. Yang, A. Yang, et al.

► To cite this version:

V. Reux, Laurent Calvez, S. Billon, A. Gautier, H.-L. Ma, et al.. High refractive index IR lenses based on chalcogenide glasses molded by spark plasma sintering. *Optical Materials Express*, 2021, 11 (6), pp.1622-1630. 10.1364/OME.427686 . hal-03249506

HAL Id: hal-03249506

<https://hal.science/hal-03249506>

Submitted on 25 Oct 2021

HAL is a multi-disciplinary open access archive for the deposit and dissemination of scientific research documents, whether they are published or not. The documents may come from teaching and research institutions in France or abroad, or from public or private research centers.

L'archive ouverte pluridisciplinaire **HAL**, est destinée au dépôt et à la diffusion de documents scientifiques de niveau recherche, publiés ou non, émanant des établissements d'enseignement et de recherche français ou étrangers, des laboratoires publics ou privés.



Distributed under a Creative Commons Attribution 4.0 International License



High refractive index IR lenses based on chalcogenide glasses molded by spark plasma sintering

VALENTIN REUX,¹ LAURENT CALVEZ,^{1,*} SÉBASTIEN BILLON,¹ ANTOINE GAUTIER,¹ HONGLI MA,¹ PATRICK HOUIZOT,² FRÉDÉRIC CHARPENTIER,³ HUGUES TARIEL,³ ZHIYONG YANG,⁴  ANPING YANG,⁴ AND XIANG-HUA ZHANG¹

¹Univ Rennes, CNRS, ISCR (Institut des Sciences Chimiques de Rennes) - UMR 6226, F-35000 Rennes, France

²Institut de Physique de Rennes, IPR, UMR URI-CNRS 6251, Université de Rennes 1, 35042 Rennes Cedex, France

³Diafir, Avenue Chardonnet, Parc Lorans, 35000 Rennes, France

⁴Jiangsu Key Laboratory of Advanced Laser Materials and Devices, School of Physics and Electronics Engineering, Jiangsu Normal University, Xuzhou, Jiangsu 221116, China

*Corresponding author: laurent.calvez@univ-rennes1.fr

Abstract: In this work, spark plasma sintering is used to mold non conventional chalcogenide glasses of high refractive index at low temperature (<400°C). This equipment, usually used for sintering refractory materials, is presented as efficient for both densification and high precision molding of IR transparent bulks and lenses of telluride glasses. Thermo-mechanical and optical characteristics of the selected Ge₂₅Se₁₀Te₆₅ glass composition were investigated showing a refractive index of 3,12@10 μm and with however a limited resistance to crystallization. Mechanical milling of raw Ge, Se, Te elements leads to a major amorphous phase with the formation of a small proportion of GeTe crystals. Remaining GeTe crystals induce a fast crystallization rate during the sintering process leading to the opacity of the material. SPS flash moldings were then performed using melt quenched glass powders to produce complex lenses. It has been found that the critical parameter to reach optimal IR transparency is mainly the powder granulometry, which should be superior to 100 μm to prevent from MIE scatterings. The possibility of producing high refractive index infrared lenses has been demonstrated even with unstable glasses against crystallization.

© 2021 Optical Society of America under the terms of the [OSA Open Access Publishing Agreement](#)

1. Introduction

The chalcogenide glasses are known to be an important class of advanced functional material for various applications in the photonic field: thermal imaging [1–4], biomedical sensors [5–7], solid state batteries [8]. . . Since several decades, this family of glass represents a cost effective alternative to single-crystalline germanium or polycrystalline ZnSe for IR optics. The commercial demand for low cost thermal cameras is still growing and has exploded in 2020 due to the worldwide pandemic [9]. Thus, even if they present weaker mechanical properties, some low-cost glass compositions free of germanium such as As₂Se₃ attract a growing interest. However the final cost of IR optics, especially small-size optics, is mainly governed by the synthesis and processing instead of raw materials. In fact, glass ingots of big diameter (about 20cm) are produced in high volume and discs are obtained by first coring and then cutting. In the next step, glass slices are molded above T_g to final shape for making high precision IR optics. The coring process could induce a material loss higher than 30%, which can only partially be reused as starting materials. In this context, developing a process that allows for making a near-shape or

even finished IR optics by using residual glass may be of high interest. Our study is dedicated to a promising novel glass with the optimized composition of $\text{Ge}_{25}\text{Se}_{10}\text{Te}_{65}$. The optical and thermo-mechanical properties of this novel glass which present a high refractive index ($n > 3$) will be characterized, highlighting its ability to be used as IR lenses materials for low-cost, large field of view and compact IR systems. In the case of complex objectives (three lens systems, zoom etc . . .) the lenses of high refractive index could have higher optical power and be lighter.

2. Experimental details

Bulk glass slices of $\text{Ge}_{25}\text{Se}_{10}\text{Te}_{65}$ glass composition were prepared by the classical melt-quenching method in silica tubes. Raw materials (Ge, Se, Te) of 5N purity were melted at 750°C for 12 h in a silica ampoule placed under vacuum before being quenched in water and annealed 10°C below T_g to relax mechanical constrains. Obtained glass rods were cut into slices of different thicknesses that were polished on both sides for optical and mechanical measurements. The transmission of melt quenched samples serve as a reference.

In parallel, Mechanical milling was performed with a Restsch Planetary ball mill PM100. Raw materials (Ge,Se,Te) of 5N purity were put in a 125 mL WC bowl with 6 WC balls of a diameter of 20 mm. A ball:powder mass ratio of 18.75:1 was used. Rotations at 400 rpm for 3 min and 3 min pauses were alternated for several hours. Obtained powders were characterized by DRX and DSC.

Near-shape sintered chalcogenide glasses were prepared by introducing a calculated amount of glass powder into a die of adequate diameter. Preliminary experiments of densification of the GeSeTe glass composition were performed on FCT group (model HPD10) SPS to obtain blanks (parallel and flat slices). 1.5 g of powder obtained by mechanical milling or by hand-grinding from melt-quenched glasses were heated up to 230°C (40°C above T_g) under a pressure of 63 MPa (5kN) for 3 minutes under vacuum (10^{-2}Pa). Dies of 10 mm diameter, protected by an inner foil of papyex and aluminum were used. Aluminum blocks were added on the piston as a carbon diffuser barrier.

Glass density was measured on an average of 5 measurements using the Archimedes method by submerging samples in water. Hardness and toughness were determined using a Vickers microindenter MATZUZAWA on an average of 12 measures, with a charge of 100 g for 5s. Young's modulus, shear modulus and Poisson's ratio was obtained by measuring the ultrasound propagation speed in the glass.

The optical properties in the infrared region were measured using a spectrophotometer Bruker Tensor 37 FTIR. The refractive index in the 1.7-20 μm range was measured on single-side polished glass disc ($\text{Ø}15\text{ mm}$) by an IR variable angle spectroscopic ellipsometer (IR-VASE, J.A. Woollam, Lincoln, NE). Infrared pictures were recorded using a FLIR IR working in the 8-12 μm region. Pictures were recorded using a Keyence optical microscope. Thermal properties of the powder were analyzed by differential scanning calorimetry TA Instruments Q20 (New Castle, DE) using a ramp of $10^\circ\text{C}/\text{min}$. X-ray diffraction measurements were performed on a Malvern Panalytical X'pert Pro diffractometer. Two types of programs were used: routine acquisition, with a step of 0.026° and 40s by step, and long-time acquisition, with the same step and 400s by step. Grain size was measured using a Fritsch analysette 22 nanotec laser particle sizer.

3. Results

Nowadays the most common IR lenses available on the market are based on As_2Se_3 ($n=2.81$ (@1.5 μm) [10]) and Ge-As-Se glasses ($n=2.75$ (@10 μm) [11]). High refractive index will lead to high optical power, therefore thinner and lighter lenses. The Table 1 lists some glass compositions having high refractive index with their characteristic temperatures.

For industrial applications, ideal compositions should both present a high refractive index, a glass transition temperature above 180°C and a good thermal stability (highest difference of

Table 1. Composition and properties of some chalcogenide glasses with high refractive index

| Composition | n (wavelength) | Tg(°C) | Tx(°C) | Ref. |
|--|----------------|--------|--------|---------|
| Ga ₁₀ Ge ₁₅ Te ₇₅ | 3,39 (10μm)* | 172 | 285 | [12] |
| Ge ₂₀ Se ₂ Te ₇₈ | 3,42 (8μm) | 153 | 250 | [13,14] |
| Ge ₂₀ Se ₁₀ Te ₇₀ | 3,26 (8μm) | 156 | 236 | [13,14] |
| Ge ₂₀ Se ₆₀ Te ₂₀ | 2,55 (8μm) | 188 | 405 | [13,15] |
| Ge ₂₀ Se ₇₀ Te ₁₀ | 2,5 (8μm) | 175 | 430 | [13,15] |
| Ge ₂₅ Se ₁₀ Te ₆₅ | 3,2 (6-7μm) | 189 | 340 | [15,16] |

temperature between Tx and Tg) in order to be easily shaped. In line with the previous table, glasses belonging to the Ge-Se-Te system are a good compromise, thus our work was focused on the Ge₂₅Se₁₀Te₆₅ glass composition.

The Ge₂₅Se₁₀Te₆₅ glass has a Tg of 189°C and a small crystallization peak at around 260°C. This glass presents a density of 5.35 ± 0.02 g/cm³ and a hardness of 140 ± 5 Hv. It has a Young's modulus of 19.8 ± 2 GPa, a shear modulus of 7.8 GPa and a Poisson's ratio of 0.268 ± 0.01 .

As shown in Fig. 1(a), its transmission ranges from 2 to 17 μm. An absorption band at 12.8 μm corresponding to the Ge-O bond vibrations is observed in the base glass. Chalcogenide glasses can be purified using different processes [12,17]. In this study, an additional purification step is proceeded by adding 100 ppm of Mg to the raw elements before melting, leading to the removal of absorption bands. One can see in Fig. 1(b) that this glass presents a refractive index slightly lower than the value presented in the bibliography. At a wavelength of 6 μm, Peng et al. measured a refractive index of 3.23, where we find the value of 3.127.

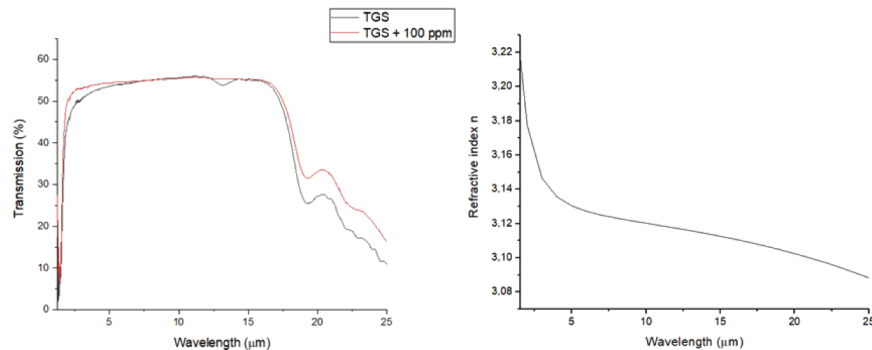


Fig. 1. Transmission spectra of TGS base glass and TGS glass purified with 100 ppm of Mg (left), measured refractive index of base glass (right).

4. Mechanical milling

Reaction between elements and their amorphization process are progressive, starting with Se (JCPDS file n°00-047-1514) that can form a glass by itself [18] and then Te (JCPDS file n°01-079-0736). As observable in Fig. 2, after 25 h of milling only diffraction peaks due to crystalline Ge (JCPDS file n°01-089-2768) are still visible. Chemical reaction of raw Ge presents a slow kinetic due to its high hardness (6 on the Mohs scale) and the strong Ge-Ge bond, as demonstrated in previous studies [18–20]. This diffraction peak gradually decreases with increasing milling time up to its disappearance. However, diffraction measurements with increased time of acquisition (0.026° step, 400s by step) show a residual crystalline Ge peak. Then, crystalline GeTe (JCPDS file n°00-047-1079) phase appears after 56 h of milling. It is important to note that the identical

milling process applied on a sample synthesized by melt-quenching also leads to the apparition of a similar crystalline phase by 20 min of milling. One can assume that the high energy due to high milling rotation speed and the use of heavy WC balls and bowl induces the powder reaching the crystallization temperature ($T_x = 260^\circ\text{C}$) locally.

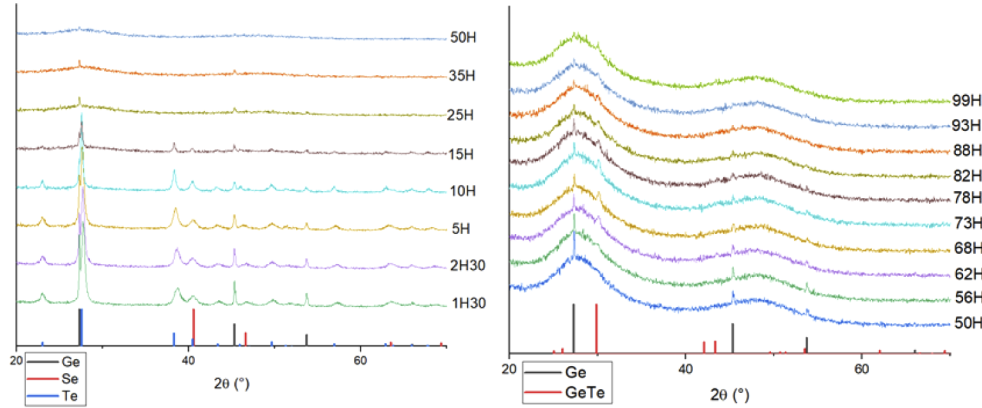


Fig. 2. X-Ray Diffraction of powders obtained after different milling time. Routine acquisition (left) and long-time acquisition (right).

In Fig. 3, one can observe a glass transition temperature (T_g) of 180°C at different times of milling. This T_g is relatively close to the one of the reference glass (189°C) obtained by melt-quenching. The DSC curves show evidences of the presence of several crystallized phases, which seems not to be affected by the duration of milling. Two main T_x are observed, at around 240°C (T_{x1}) and 300°C (T_{x2}) and are attributed to the crystallization of Te and GeTe respectively [21]. Differences of DSC curves is explained by the differences on the morphology and the thermal history of the analyzed powders. The powder obtained by mechanical milling has higher specific surface and nucleation can happen during the ball milling

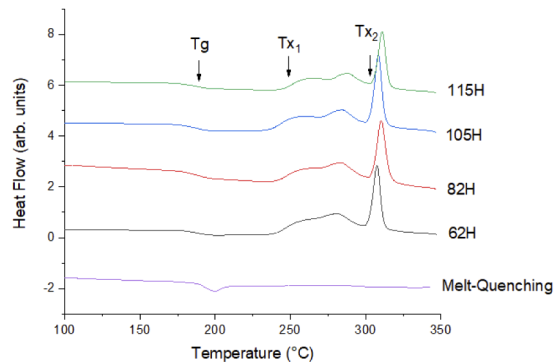


Fig. 3. DSC of melt-quenched bulk and powder obtained by mechanical alloying after 62 h, 82 h, 105 h and 115 h.

The size dispersion of mechanically milled powder is presented in Fig. 4. The particle size ranges from several hundred of nanometers up to $70\ \mu\text{m}$. Two populations can be mainly distinguished with maxima at $2\ \mu\text{m}$ and $20\ \mu\text{m}$. The phi 50 and phi 90 are respectively $7.405\ \mu\text{m}$ and $25.484\ \mu\text{m}$

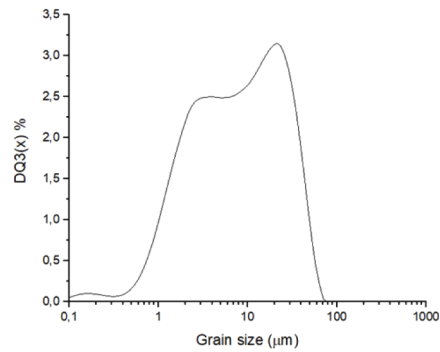


Fig. 4. Measured grain size after 88 h of milling.

5. SPS sintering

First experiments of Spark Plasma Sintering were focused on mechanical milled powder of $\text{Ge}_{25}\text{Se}_{10}\text{Te}_{65}$ glass as presented above. However, powder obtained by mechanical milling contains residual crystalline GeTe in small proportion in addition to major amorphous phase. While a small proportion of crystals within glass-ceramics could be of great interest to enhance mechanical properties [22], the particle size must be controlled to avoid excessive optical losses in the IR bands due to scatterings. About 1.5 g of powder was sintered by SPS at 230°C , $T_g+40^\circ\text{C}$, for 3 minutes. Even if the step is short and the temperature of sintering limited, Delaizir et al. demonstrated that the crystallization process can be strongly accelerated under pressure. In our case, even if the compactness reached is high ($>98\%$), due to the induced scattering, all attempts provide an opaque sample to the IR camera.

Therefore, it was concluded that the SPS sintering process of ball milled glass powders containing even a small amount of crystallites, would lead to uncontrollable crystallization of the sintered sample as shown in Fig. 5, and the obtained samples were typically opaque.

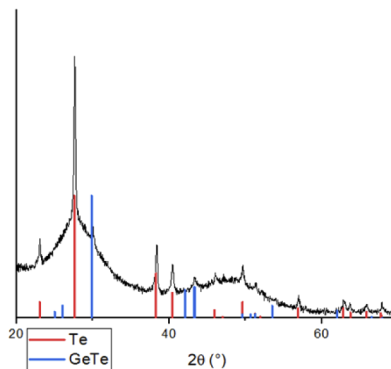


Fig. 5. X-Ray diffraction of sample obtained by sintering powder obtained by ball milling.

Then, melt-quenching glasses have been used and hand grounded glass powder have been sieved to obtain two population of powder size: below and above $100\ \mu\text{m}$. A similar sintering procedure as described above was used to obtain IR transparent bulk glasses by Spark Plasma Sintering. Table 2 presents the relative density of sintered samples compared to the base. Whatever the powder size, the compactness is higher than 99% , which is necessary for IR applications. In fact,

considering the precision of the measurements, the density of the sintered samples is really close to the one of the base glass.

Table 2. Measured density and relative density of base glass and sintered results for both powders

| Sample | Density (g/cm ³) | Relative density (%) |
|------------|------------------------------|----------------------|
| Base glass | 5.35 center0.02 | 100 |
| <100 | 5.31 center0.02 | 99.2 |
| >100 | 5.32 center0.02 | 99.4 |

As shown in Figs. 6 and 7, infrared transparency of sintered samples of both powders have been characterized by FTIR, from 1,25 μm up to 25 μm (Fig. 6) and visualized through thermal camera working in the 8-12 μm region (Fig. 7).

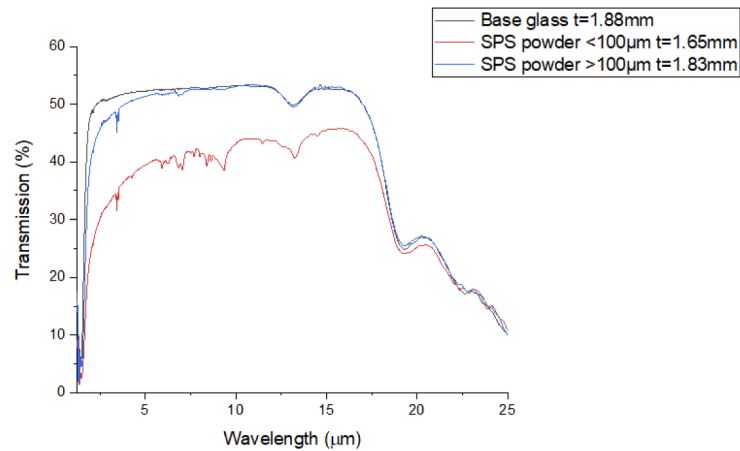


Fig. 6. Transmission spectra of the base glass synthesized by melt-quenching and of samples obtained by SPS sintering of powder <100 μm and powder >100 μm .

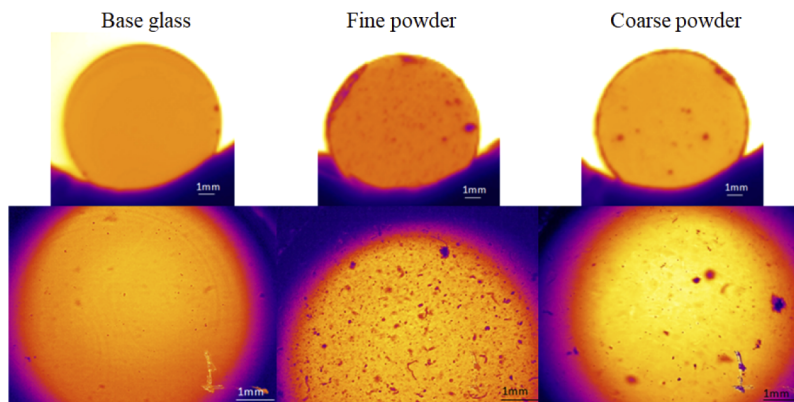


Fig. 7. IR image (up) and zoomed IR images (down) of base glass and sintered sample obtained with different grain size powders.

Transmission of the sintered sample with powder >100 μm is identical to the base glass from approximately 5 μm up to 25 μm , presenting small scatterings in the short wavelength. The

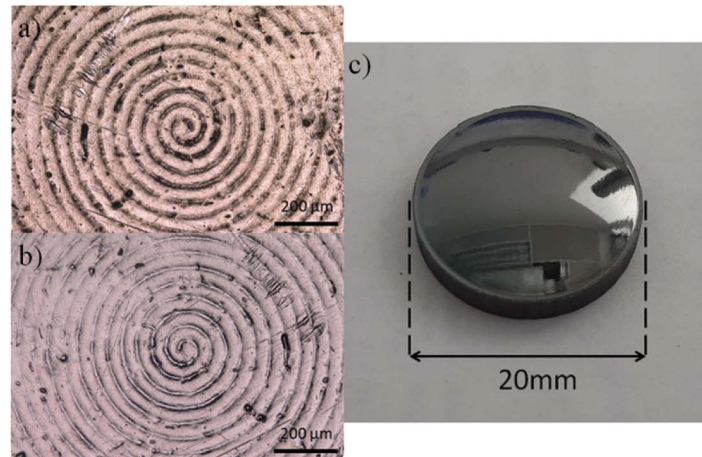


Fig. 8. Pictures taken by optical microscopy of aluminum block (a), resulting footprint from the aluminum block on TGS lens (b) and full lens after molding (c).

sample obtained with more fine powder ($<100\ \mu\text{m}$) gives a lower transmission around 46%, with, in addition, the presence of multiples absorptions in the range $6-10\ \mu\text{m}$.

As observable in Fig. 7, the base glass contains some small bubbles only visible by zooming on the bulk. Sintered samples presents some impurities (black dots) that are usually dusts ($<10\ \mu\text{m}$) and carbon contamination ($\approx 100\ \mu\text{m}$). Most of them are visible in the sintered sample using relatively fine powder having a size $<100\ \mu\text{m}$. The high volume percentage of impurities, even if their size is maintained lower than $100\ \mu\text{m}$, induces strong Mie scatterings that affect the whole IR transparency. Fine powders are also chemically more active/reactive, which can explain the additional absorption peaks in the $5-10\ \mu\text{m}$ wavelength region due to the absorbed/adsorbed impurities during the processing.

The use of coarse powder allows for removing most of the carbon impurities. The Rayleigh scatterings provoking the small of transparency in the short wavelength is mainly governed by residual pores of tens of nanometers size.

In order to demonstrate the feasibility of molding complex IR optical lenses with the $\text{Ge}_{25}\text{Se}_{10}\text{Te}_{65}$ glass, aluminum footprints of spherical lenses shape were produced. A similar process (T, t, P) was used for sintering powder leading to a lens of 3 mm thick and 20 mm diameter transparent in the IR range (Fig. 8(c)). The surface details of the footprints are perfectly reproduced onto the lens surface as observable by microscope observation (Fig. 8(a), (b)). The spacing and depth of the furrows on the footprints and on the glass surface are of $48\ \mu\text{m}$ and $1,5\ \mu\text{m}$ respectively. This result highlights the great ability of molding complex shape of unstable chalcogenide glasses by Spark Plasma Sintering.

It is interesting to point out that $\text{Ge}_{25}\text{Se}_{10}\text{Te}_{65}$ glasses of maximum 13 mm diameter can be synthesized by melt-quenching method due to their tendency to crystallization. The use of ground powder is an efficient way to produce complexes and much bigger lenses.

6. Conclusion

Glasses with high refractive index and good transparency in the $8-12\ \mu\text{m}$ region mainly belong to the Ge-Ga-Te and Ge-Se-Te ternary systems. The $\text{Ge}_{25}\text{Se}_{10}\text{Te}_{65}$ glass composition was selected as the best compromise of thermal, mechanical and optical properties for IR optical applications. Mechanical milling performed on Ge, Se, Te raw materials lead to a progressive amorphization of the mixture while GeTe crystals are formed in the meantime. These crystals induce strong

scatterings after SPS sintering, provoking the glass opacity in the infrared range. However, by using flash SPS sintering, the possibility to rapidly and reproducibly shape lenses from raw powder of the relatively unstable $\text{Ge}_{25}\text{Se}_{10}\text{Te}_{65}$ glass against crystallization was demonstrated. The obtained bulk glasses present an identical transparency to the reference glass in the 3rd optical window. The use of coarse powder having a size superior to 100 μm is beneficial to obtain perfect transmission in the 8-14 μm region while keeping a high transparency in the 3-5 μm . This work paves the way to the production of high refractive index infrared lenses even with unstable glasses against crystallization.

Funding. Electronic Components and Systems for European Leadership (826131); European Regional Development Fund; Ministère de l'Éducation Nationale, de l'Enseignement Supérieur et de la Recherche; Région Bretagne; Rennes Métropole; Institut Universitaire de France.

Acknowledgements. This work is part of a project that has received funding from the ECSEL Joint Undertaking (JU) under grant agreement No 826131. The JU receives support from the European Union's Horizon 2020 research and innovation programme and France, Germany, Ireland, Italy. Completed by local funding from the French region Auvergne Rhône Alpes. This publication is supported by the European Union through the European Regional Development Fund (ERDF), the Ministry of Higher Education and Research, the French region of Brittany and Rennes Métropole. Authors also would like to acknowledge the IUF (Institut Universitaire de France).

Disclosures. The authors declare no conflicts of interest related to this article.

Data availability. No data were generated or analyzed in the presented research.

References

1. L. Calvez, "Chalcogenide glasses and glass-ceramics: transparent materials in the infrared for dual applications," *C. R. Phys.* **18**(5-6), 314–322 (2017).
2. J.-L. Adam, L. Calvez, J. Trolès, and V. Nazabal, "Chalcogenide glasses for infrared photonics," *Int. J. Appl. Glass Sci.* **6**(3), 287–294 (2015).
3. F. Chenard, O. Alvarez, and A. Buff, "Chalcogenide glass materials for novel infrared optics," in *Advanced Photonics 2018 (BGPP, IPR, NP, NOMA, Sensors, Networks, SPPCom, SOF) (2018), Paper NoTu4D.2* (Optical Society of America, 2018), p. NoTu4D.2.
4. E. Lavanant, E. Lavanant, L. Calvez, F. Cheviré, M. Rozé, T. Hingant, R. Proux, Y. Guimond, and X.-H. Zhang, "Radial gradient refractive index (GRIN) infrared lens based on spatially resolved crystallization of chalcogenide glass," *Opt. Mater. Express* **10**(4), 860–867 (2020).
5. J. Charrier, M.-L. Brandily, H. Lhermite, K. Michel, B. Bureau, F. Verger, and V. Nazabal, "Evanescent wave optical micro-sensor based on chalcogenide glass," *Sens. Actuators, B* **173**, 468–476 (2012).
6. M.-L. Anne, J. Keirsse, V. Nazabal, K. Hyodo, S. Inoue, C. Boussard-Pledel, H. Lhermite, J. Charrier, K. Yanakata, O. Loreal, J. Le Person, F. Colas, C. Compère, and B. Bureau, "Chalcogenide glass optical waveguides for infrared biosensing," *Sensors* **9**(9), 7398–7411 (2009).
7. P. Lucas, G. J. Coleman, C. Cantoni, S. Jiang, T. Luo, B. Bureau, C. Boussard-Pledel, J. Troles, and Z. Yang, "Chalcogenide glass sensors for bio-molecule detection," in *Optical Fibers and Sensors for Medical Diagnostics and Treatment Applications XVII* (International Society for Optics and Photonics, 2017), Vol. 10058, p. 100580Q.
8. M. Tatsumisago and A. Hayashi, "19 - Chalcogenide glasses as electrolytes for batteries," in *Chalcogenide Glasses*, J.-L. Adam and X. Zhang, eds. (Woodhead Publishing, 2014), pp. 632–654.
9. "Infrared Thermometer Market by Type, Component, Application, End-Use | COVID-19 Impact Analysis | MarketsandMarketsTM," <https://www.marketsandmarkets.com/Market-Reports/infrared-thermometer-market-191167475.html>.
10. A. Novikova, "Élaboration d'optiques infrarouges par combinaison de la mécanosynthèse et du frittage SPS," thesis, Rennes 1 (2018).
11. H. G. Dantanarayana, N. Abdel-Moneim, Z. Tang, L. Sojka, S. Sujecki, D. Furniss, A. B. Seddon, I. Kubat, O. Bang, and T. M. Benson, "Refractive index dispersion of chalcogenide glasses for ultra-high numerical-aperture fiber for mid-infrared supercontinuum generation," *Opt. Mater. Express* **4**(7), 1444–1455 (2014).
12. S. Zhang, X. Zhang, M. Barillot, L. Calvez, C. Boussard, B. Bureau, J. Lucas, V. Kirschner, and G. Parent, "Purification of $\text{Te}_{75}\text{Ga}_{10}\text{Ge}_{15}$ glass for far infrared transmitting optics for space application," *Opt. Mater.* **32**(9), 1055–1059 (2010).
13. S. Mauriceon, C. Boussard-Pledel, J. Troles, A. J. Faber, P. Lucas, X. H. Zhang, J. Lucas, and B. Bureau, "Telluride Glass Step Index Fiber for the far Infrared," *J. Lightwave Technol.* **28**(23), 3358–3363 (2010).
14. S. Mauriceon, B. Bureau, C. Boussard-Pledel, A. J. Faber, X. H. Zhang, W. Geliesen, and J. Lucas, "Te-rich Ge–Te–Se glass for the CO₂ infrared detection at 15 μm ," *J. Non-Cryst. Solids* **355**(37-42), 2074–2078 (2009).
15. D. J. Sarrach, J. P. De Neufville, and W. L. Haworth, "Studies of amorphous GeSeTe alloys (I): Preparation and calorimetric observations," *J. Non-Cryst. Solids* **22**(2), 245–267 (1976).

16. X. Peng, L. Jiang, G. Li, Y. Yuan, Y. Wang, S. Dai, N. Zhang, J. Su, P. Yang, and P. Zhang, "Fabrication and characterization of multimaterial $\text{Ge}_{25}\text{Se}_{10}\text{Te}_{64}/\text{As}_2\text{S}_3$ chalcogenide fiber with a high value of the numerical aperture," *J. Non-Cryst. Solids* **525**, 119690 (2019).
17. L. Calvez, H. L. Ma, J. Lucas, and X. H. Zhang, "Glasses and glass-ceramics based on GeSe_2 - Sb_2Se_3 and halides for far infrared transmission," *J. Non-Cryst. Solids* **354**(12-13), 1123–1127 (2008).
18. E. Petracovschi, M. Hubert, J.-L. Adam, X.-H. Zhang, and L. Calvez, "Synthesis of GeSe_4 glass by mechanical alloying and sintering," *Phys. Status Solidi B* **251**(7), 1330–1333 (2014).
19. M. Hubert, E. Petracovschi, X.-H. Zhang, and L. Calvez, "Synthesis of Germanium–Gallium–Tellurium (Ge–Ga–Te) ceramics by ball-milling and sintering," *J. Am. Ceram. Soc.* **96**(5), 1444–1449 (2013).
20. B. Xue, L. Calvez, M. Allix, G. Delaizir, and X.-H. Zhang, "Amorphization by mechanical milling for making IR transparent glass-ceramics," *J. Am. Ceram. Soc.* **99**(5), 1573–1578 (2016).
21. I. U. Arachchige, R. Soriano, C. D. Malliakas, S. A. Ivanov, and M. G. Kanatzidis, "Amorphous and crystalline GeTe nanocrystals," *Adv. Funct. Mater.* **21**(14), 2737–2743 (2011).
22. M. Rozé, L. Calvez, M. Hubert, P. Toupin, B. Bureau, C. Boussard-Plédel, and X.-H. Zhang, "Molded glass-ceramics for infrared applications," *Int. J. Appl. Glass Sci.* **2**(2), 129–136 (2011).